

Geomorphological evidence for ground ice on dwarf planet Ceres

Britney E. Schmidt^{1*}, Kynan H. G. Hughson², Heather T. Chilton¹, Jennifer E. C. Scully³, Thomas Platz⁴, Andreas Nathues⁴, Hanna Sizemore⁵, Michael T. Bland⁶, Shane Byrne⁷, Simone Marchi⁸, David P. O'Brien⁵, Norbert Schorghofer⁹, Harald Hiesinger¹⁰, Ralf Jaumann¹¹, Jan Hendrik Pasckert¹⁰, Justin D. Lawrence¹, Debra Buzckowski¹², Julie C. Castillo-Rogez³, Mark V. Sykes⁵, Paul M. Schenk¹³, Maria-Cristina DeSanctis¹⁴, Giuseppe Mitri¹⁵, Michelangelo Formisano¹⁴, Jian-Yang Li⁵, Vishnu Reddy⁵, Lucille LeCorre⁵, Christopher T. Russell² and Carol A. Raymond³

Five decades of observations of Ceres suggest that the dwarf planet has a composition similar to carbonaceous meteorites and may have an ice-rich outer shell protected by a silicate layer. NASA's Dawn spacecraft has detected ubiquitous clays, carbonates and other products of aqueous alteration across the surface of Ceres, but surprisingly it has directly observed water ice in only a few areas. Here we use Dawn Framing Camera observations to analyse lobate morphologies on Ceres' surface and we infer the presence of ice in the upper few kilometres of Ceres. We identify three distinct lobate morphologies that we interpret as surface flows: thick tongue-shaped, furrowed flows on steep slopes; thin, spatulate flows on shallow slopes; and cusped sheeted flows that appear fluidized. The shapes and aspect ratios of these flows are different from those of dry landslides—including those on ice-poor Vesta—but are morphologically similar to ice-rich flows on other bodies, indicating the involvement of ice. Based on the geomorphology and poleward increase in prevalence of these flows, we suggest that the shallow subsurface of Ceres is comprised of mixtures of silicates and ice, and that ice is most abundant near the poles.

Ceres has a dark, hydrated surface^{1–3} and its shape and low density suggest an ice-rich^{4–6} or hydrated composition⁷. Measurements of its shape are inconsistent with a porous interior, indicating some degree of partial differentiation^{4–6,8}. Dawn measurements of Ceres' internal structure are consistent with a lower density outer layer of 1,680–1,950 kg m⁻³ and interior silicate core⁸, suggesting that early accretionary heating led to some degree of convection, creating water–rock reactions and forming an ice-rich outer layer but not a pure ice shell. This thermal cycling would drive water from the interior, where impacts into or failures at the surface could expose ice. Dawn's Gamma Ray and Neutron Detector (GRaND) detected an ice table on Ceres within 1 m of the surface at the equator and at the surface near the poles⁹.

A one-time detection of OH emission near Ceres' poles¹⁰ and recent observations of water emission from Ceres¹¹, along with potential activity at Occator crater¹² and water ice in Oxo crater¹³, burgeon the case for ice within Ceres' shallow subsurface. Images from Dawn's Framing Camera¹⁴ reveal that Ceres is not bereft of craters^{15,16}, in contrast with pre-Dawn expectations that craters would be relaxed or erased by an ice mantle^{4,17}. Paradoxically, these craters follow the same scaling relationships as those on the icy

satellites rather than those of ice-poor bodies. Although unlikely on its surface at low latitude due to solar insolation, ice can endure in Ceres' subsurface over billions of years if protected by an insulating layer^{18–20}; the necessary burial depth may be less than 1 m above ~40° latitude since its obliquity is low²⁰. Thus, intimate mixtures of ice and rock, silicates with pore-filling ice, and ice deposits are possible in its upper layers. Without an atmosphere, any ice must result from ice cycling through Ceres by endogenic and exogenic processes. This ice would be deposited differently but be physically similar to ice-silicate materials in the surfaces of other planetary bodies, including the Earth, and thus we adopt the standard term 'ground ice' to refer to these mixtures. Because mass wasting occurs when material within the upper few kilometres is destabilized, we analysed clear filter Framing Camera images of flows on Ceres in an effort to characterize the nature of Ceres' surface and shallow subsurface materials.

Observations of mass wasting on Ceres

Mass wasting on Ceres is usually related to impact craters as these are its primary topographic features. Large-scale flows associated with craters are the most common features, and are found in much

¹Georgia Institute of Technology, Atlanta, Georgia 30332, USA. ²University of California at Los Angeles, Los Angeles, California 90095-1567, USA. ³Jet Propulsion Laboratory, California Institute of Technology, Pasadena, California 91109, USA. ⁴Max-Planck Institut für Sonnensystemforschung, Göttingen 37077, Germany. ⁵Planetary Science Institute, Tucson, Arizona 85719-2395, USA. ⁶United States Geological Survey, Flagstaff, Arizona 86001, USA. ⁷University of Arizona, Tucson, Arizona 85721-0092, USA. ⁸Southwest Research Institute, Boulder, Colorado 80302, USA. ⁹University of Hawaii at Manoa, Honolulu, Hawaii 96822, USA. ¹⁰Institut für Planetologie, Westfälische Wilhelms-Universität, Münster 48149, Germany. ¹¹German Aerospace Center (DLR), Berlin 12489, Germany. ¹²Applied Physics Laboratory, Johns Hopkins University, Laurel, Maryland 20723, USA. ¹³Lunar and Planetary Institute, Houston, Texas 77048, USA. ¹⁴Istituto di Astrofisica e Planetologia Spaziali, INAF, Roma 00133, Italy. ¹⁵Universite de Nantes, Nantes 44035, France. *e-mail: britneys@eas.gatech.edu

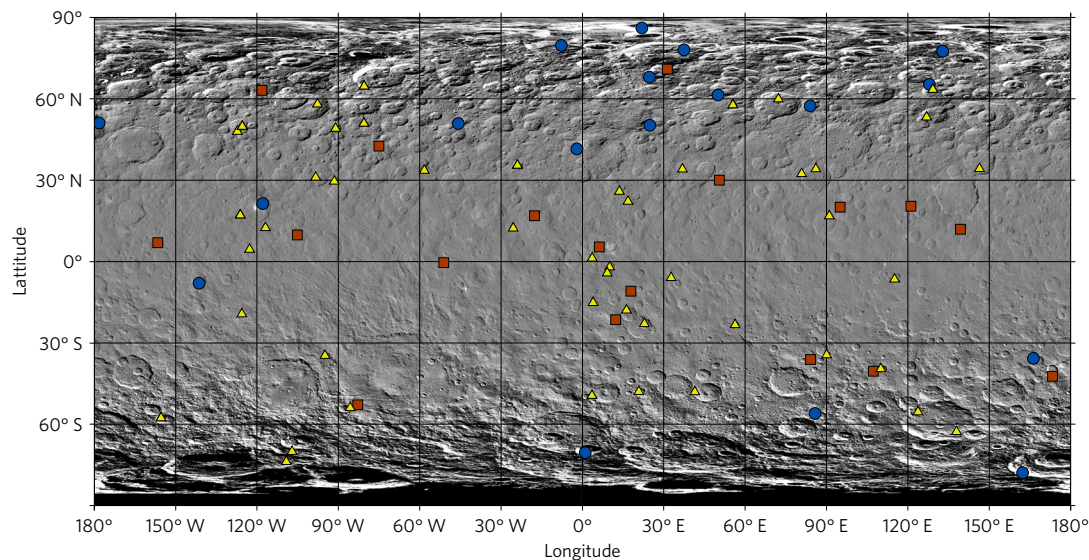


Figure 1 | Global distribution of flow features on Ceres. Flow features occur in over 20% of Ceres' craters larger than 10 km in diameter, and have a poleward positive trend in number, consistent with their behaviour being controlled by ground ice. Shown are the locations of type 1 flows, interpreted as deforming ice flows (blue circles), type 2 flows, interpreted as long runout landslides (yellow triangles) and type 3 flows, interpreted as melted or fluidized flows (red squares).

higher abundance than is typical on other bodies^{21,22}—in at least 20% of craters above 10 km in diameter. These features, marked in Fig. 1, are concentrated above 30°. There is also a slight asymmetry, with more mass wasting at northern than at southern high latitudes. This distribution implies a gradient in surface material strength, with a poleward increase in weak or easily mobilized materials.

The most striking flow morphologies are found in high-latitude craters, above ~50°. In these features, segments of crater walls fail, forming down-slope flows as shown in Fig. 2. These flows are a part of a class of features designated as 'type 1', are tongue-shaped, lobate, and voluminous, and up to hundreds of metres thick. Type 1 flows occur at a wide range of scales, but always have single or multiple elongate trunks as wide as their source, often overprinted by parallel longitudinal furrows, and exhibit broad steep snouts and distal ramparts at their termini. The largest of these features form where small impact craters are emplaced into older crater walls, and material flows into the floor of the older crater. Feature A emanates from an irregular, scalloped-rim small crater, and consists of one main trunk with two flanking flows that reach 300 m thick at the toe. Superposed lobes are observed in the centre of the structure. A tall flanking ridge suggests that the flow may have left a levee as it displaced material. Feature B has a 170-m-thick primary trunk with longitudinal and transverse furrows and flanking ridges. The terminal rampart is thicker than the centre of the flow, indicating possible deflation. Feature C is a shorter, steeper flow formed by a complex of short trunks that terminate in steep, lobate toes of ~170 m thickness. In smaller flows such as those within Oxo (Supplementary Fig. 1), the source is the crater rim. Thus, although some type 1 flows could be triggered during an impact, others may form later.

The most common mass wasting on Ceres is in the form of long, spatulate, sheeted flows. These features initiate near the crests of crater rims, and generally flow down the exteriors of craters. These 'type 2' flows have circular to lobate toes, and can range in appearance from single broad or fan-shaped sheets to many sheets diverted or dispersed in multiple directions. Type 2 flows generally blanket low-grade relief, but their paths are controlled by local topography, even becoming channelized, as shown in Fig. 3. Type 2 flows traverse path lengths of tens of kilometres, on shallow slopes usually less than ten degrees. In comparison to type 1 flows,

type 2 flows appear to be less coherent, lack steep snouts, appear on shallower slopes and on outward- rather than inward-facing crater walls, and show no strong correlation with crater size. Although type 2 flows initiate at crater rims, they are morphologically distinct from ejecta and do not necessarily form contemporaneously, suggesting landslide-like behaviour, post-impact.

Cusped, sheeted flows that extend outwards from crater rims define the 'type 3' class. These features are collocated with or obscure ejecta blankets, and are characterized by thin broad sheets of smooth material that blanket local topography and terminate in layered sets of lobes or cusps. An archetype of these 'type 3' features is shown in Fig. 4. These flows are generally wider than the type 2 flows (covering > ~20% of the crater rim) but similar in thickness (tens of metres). Type 3 flows have narrow to acute curvilinear toes, lack deep longitudinal furrows, and possess lahar-like smooth to striated or hummocky textures, giving the impression of fluidization. Type 3 flows are associated with complex craters, and generally those wider than 20 km.

Comparison of flows on Ceres and other bodies

Mass wasting is common on planetary bodies, and their morphology provides a first-order indication of the processes at work. As comparisons for Ceres, we considered analogue ice-rich flows, including surface flows on the much colder surfaces of icy satellites²², on Mars, for example, refs 23–26, and the Earth, for example, refs 27–29, and on Vesta²¹ (for example, Supplementary Figs 2–4), as well as fluidized ejecta^{25–27}. Only type 3 flows are strongly coupled to impact timing or size. Rather, the variation in the source and age of the flow material, and overprinting of trunks, lobes and sheets common in type 1 and type 2 flows demonstrates they do not only form immediately post-impact.

Type 1 flows on Ceres share morphological similarities with terrestrial and Martian rock glaciers in that these flows produce thick, rounded toes, and longitudinal furrows, for example, refs 22,27,28. However, with Ceres' low gravity, it is unlikely that conditions for glacial basal slip are met, so while deformation or non-Newtonian flow within these flows could explain their morphology, flow at the bed would require reduction in basal friction (Supplementary Information). Type 2 flows share similarities to long runout landslides, with thin rounded toes, relatively long

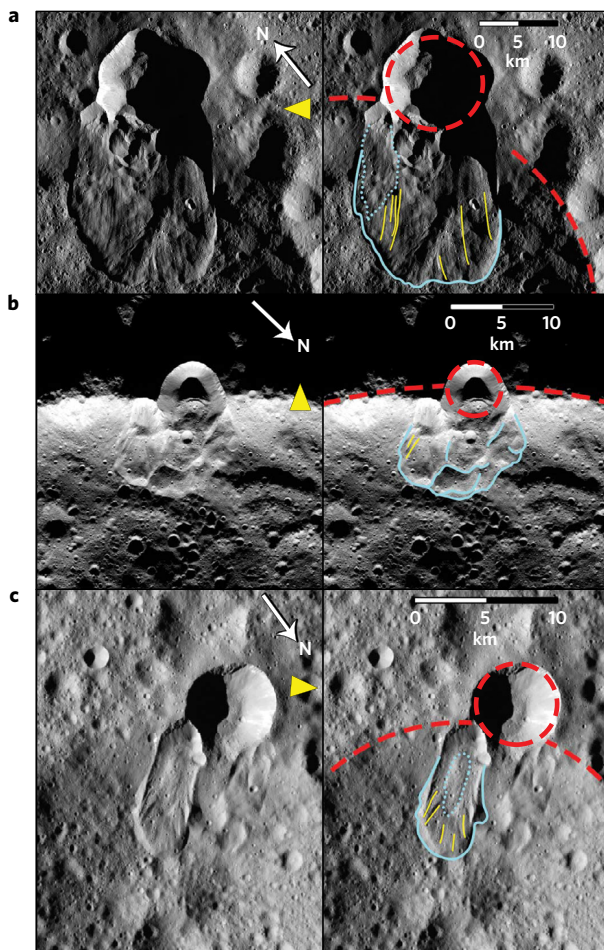


Figure 2 | Examples of type 1 flows. Type 1 flows occur primarily at Ceres' high latitudes. The direction of North and incident light are given. Blue solid lines show flow margins. Dotted blue lines trace overprinting flows. Red dashed lines delineate craters. Yellow lines follow furrows. **a**, The feature in Ghanan crater (79° N, 58° W) is the longest and most voluminous flow. **b**, The feature at 77° S, 181° W is highly complex, with several superposed trunks that began with slumped segments of the crater wall. **c**, The feature at 50° N, 44° W is possibly deflated, where the snout is thicker than the rest of the flow.

extends along shallow slopes, and examples of channelization by local topography. Type 3 flows are morphologically similar to fluidized ejecta in rampart craters on Mars, for example, refs 30,31 and on Ganymede³², and are always found exterior to crater rims. However, on Ceres' these only occur around part of the crater, and so are not necessarily ejecta. No such flow morphologies were found on Vesta (Supplementary Fig. 3)—which is critical since Ceres and Vesta have similar surface gravity and impact rates due to their proximity within the main asteroid belt (Supplementary Fig. 10). Flows on Ceres are thicker, more voluminous, and longer than those observed on Vesta. Vestan flows generally form flat conical deposits to the interior of craters, are rarely lobate, and never appear fluidized²¹. These contrasting morphologies indicate fundamentally different mechanisms; this is best explained by differences in rheology and likely composition, with Ceres flows containing weaker or lower melting point materials such as ices, clays or salts.

Mass flows transform gravitational potential energy into horizontal kinetic motion and heat. To constrain the nature of Ceres' surface flows, we measured their physical dimensions (Supplementary Table 1). To first order, comparing the ratio of the length (L) of the flow to the vertical distance it falls (the 'drop height' H) can

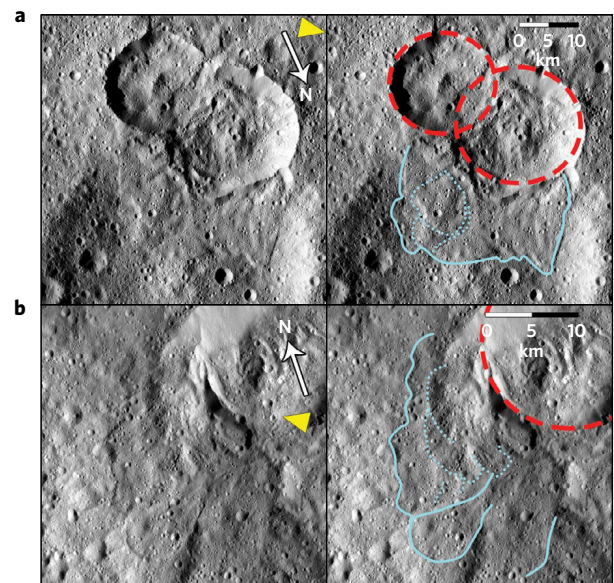


Figure 3 | Examples of type 2 flows. **a**, Cerean landslide at (53.9° N, 114° W) demonstrating typical, broad sheets with rounded (spatulate) toes up to 15.4 km long. This feature formed after the impact on the left of the figure, but originates on the rim of both craters. **b**, This landslide (18.9° N, 23.2° E) flows over a shallow 8° slope. It has two prominent lobate sheets emanating from the host crater towards the southwest, extending to 18.5 km. This feature is channelized, where the southern lobe is constrained by a ridge to the east and a crater to the south.

constrain how the flow has moved, where H/L gives the apparent internal coefficient of friction (for example, refs 22,33). The trend in H/L versus L is used to compare the efficiency of the movement among different flows. We plot these values for Ceres' flows in Fig. 5, along with reference flows on other bodies. The H/L versus L trends reveal five main points: there is no overall trend of H/L with L that defines all Cerean flows; the flows define a broad continuum; the type 2 flows are generally consistent with landslides found on Mars and Iapetus; the type 1 flows are consistent with other planetary landslides but generally form at unusually small length scales given their drop heights, and with high apparent values of internal friction; and type 3 flows show no strong trend, unlike most landslides.

In general, these data support the interpretation that there are clusters of surface flow behaviours on Ceres that define a continuum from type 1 to type 3. Type 1 flows truncate at relatively shorter lengths than the other flows and display the least efficient down-slope transport, suggesting different mechanical behaviour, such as a difference in rheology, deformation within the flow or non-Newtonian (for example, Bingham) flow³⁴. None of the trend lines shown has a strong statistical correlation and, as a group, there is no obvious relationship. On Iapetus, this same behaviour was argued as evidence for reduction in basal sliding friction by slippery ice grains²². A similar slope in H/L is found between flows on Iapetus and type 2 flows on Ceres, and for both trends, the fits are similarly poor. The type 2 H/L trend is the most similar to the Iapetus trend, and shallower than terrestrial and Martian landslides, arguing that reduction of basal friction could be occurring in Ceres flows. Type 3 flows show no obvious relationship between flow length and H/L and universally low values for H/L , which together with their collocation with impact ejecta suggests that type 3 flows result from melting and/or vaporization during energetic impacts.

The most consistent explanation for the mass wasting behaviour we observe on Ceres is ice within its shallow subsurface materials, and that variation in the ice content, surface conditions, and triggering explain the observed variations. The first spectral

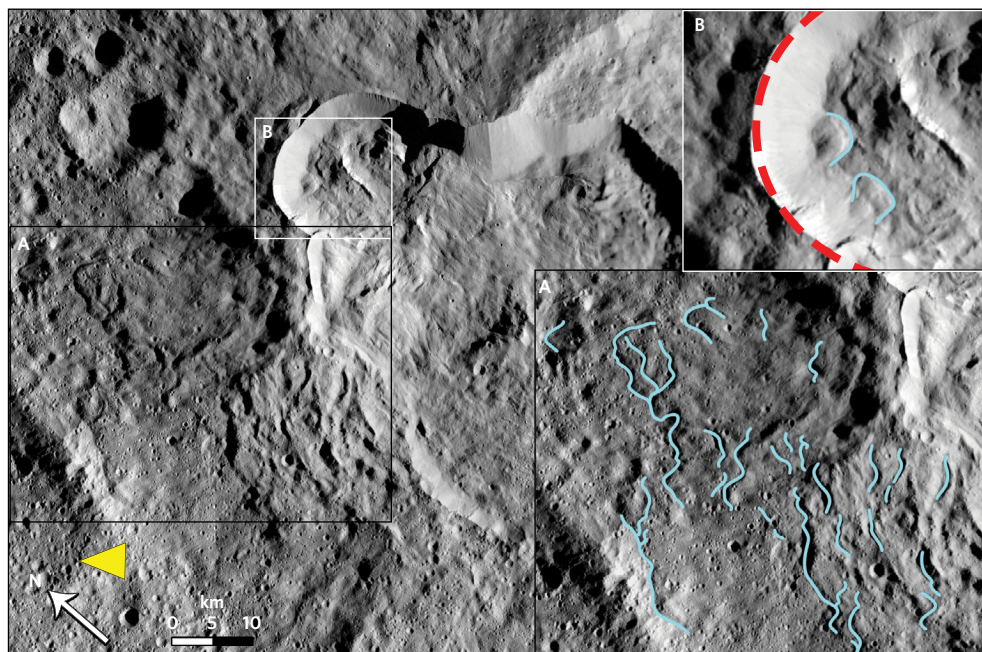


Figure 4 | Examples of type 3 flows. Type 3 flows have a platy, lobate morphology with each thin sheet comprised of smooth material, shown by this archetypal Cerean flow in Datan crater (60° N, 250° W). The black inset shows the flows in detail. Lines trace v-shaped cusped toes of the many flow sheets. The length of this flow ranges from 17–32 km. The white inset shows terracing and two lobate flows on the interior of a presumably post-impact failed rim. These landslides could represent talus cones within the crater.

detection of ice on Ceres was collocated with small type 1 flows¹³ (Supplementary Fig. 1). Type 1 features have distinct geomorphology, and lower mass transport efficiency, although they occur on steeper slopes that should promote longer flow. In particular the rolled appearance of type 1 flows, forming steep fronted snouts, is difficult to explain without deformation. Ice can creep under a wide variety of conditions^{35,36}, and such deformation or non-Newtonian flow is possible where ice content is high enough to overcome silicate grain friction (for example, ref. 34). Crater rim collapse or rapid flow down steep scarps would create high strain rates under which an ice-silicate mixture could flow or fail, explaining the observations of type 1 flows.

Type 2 flows are most consistent with lubrication by ice, which can occur at temperatures above 250 K, within a few tens of kelvin of Ceres' surface temperatures. On Ceres as on Mars and Iapetus, frictional heating of any ice grains during a landslide would raise the temperature within the flow and at its base, conditions that can cause ice to become slippery or melt. These grains reduce basal friction and allow the flow to traverse long distances even along shallow slopes^{22,33}, resulting in long, thin flows with rounded toes. Both salts and clays have lower melting points than anhydrous silicate; however, these are higher than that of ice by at least ~ 300 K. Thus, ice provides the lowest temperature threshold for mobilizing flows. We also favour ice due to several observations: detections of local surface ice from visible and infrared, and ice in the upper metre of the surface by GRaND; the lack of both long runout landslides and ice on Vesta, the surface of which primarily differs from Ceres in composition including water content; and these flows appear geographically and morphologically intermediate between cold, high-ice-content flows (type 1) and ice-melted flows (type 3). However, other long runout landslides on Earth and Mars have been attributed to an array of mechanisms, including lubrication by clay³⁷, acoustic mobilization³³, and ice in the substrate; thus, ice is not necessarily required to make type 2 landslides.

Type 3 flows are strongly correlated with impact events; they start at a crater rim but do not encircle the whole crater, suggesting that

if they are impact ejecta, either only part of the ejecta is fluidized, or these flows occur in impacts that deposit ejecta asymmetrically. Conversely, they may be flows initiated by post-impact heating or triggering. The energy required to melt subsurface ice on Ceres is easily met for most of its impactor velocity distribution, and rare faster impacts could eject up to half of this melted material³⁸.

Implications for ground ice on Ceres

Together, the dynamics and morphology of flows on Ceres are best explained by ice within its shallow subsurface; their distribution also implicates ice. Figure 6 shows the aerial density of flows on Ceres. The total number of flows per square kilometre increases above $\sim 35^{\circ}$ latitude. Although type 1 flows are rare, they generally exist above 50° , except for small flows like those in Oxo, and are the dominant flows at the poles. Although their global distribution may not uniquely require ice, Type 2 flows peak between 30° – 60° . Type 3 flows are found in low abundance, but mostly in low-mid latitudes. Thus the distribution of surface flows is consistent with a latitude-dependent depth to the ice table^{8,18–20}—with ice at or near the surface above 60° . Latitude-dependent behaviour would not be expected for salts or clays, nor has spatial variation in such compounds been observed.

Our results suggest that ice exists across Ceres in its subsurface materials, with a sharp increase above $\sim 50^{\circ}$ latitude, consistent with observations by GRaND⁸. Similar to the north–south asymmetry in the GRaND data, a north–south asymmetry is also seen in the abundance of type 1 flows. Ceres' flows occur on a spectrum consistent with the behaviour and distribution of ice, where high ice content is required for type 1 flows and melting of that ice best explains type 3 flows. Type 1 mass wasting also provides some constraint on the volume of ice possible. A minimum of 10% ice by volume is required for rock glaciers to move, although pore-filling ice is much more effective, and to flow as a fluid the volume of rock and ice must be similar, approaching 50% (refs 27–29), so ice in Ceres' upper layers may range from 10–50 vol.%. These observations make Ceres only the third planetary body where ground ice is confirmed and geographically widespread.

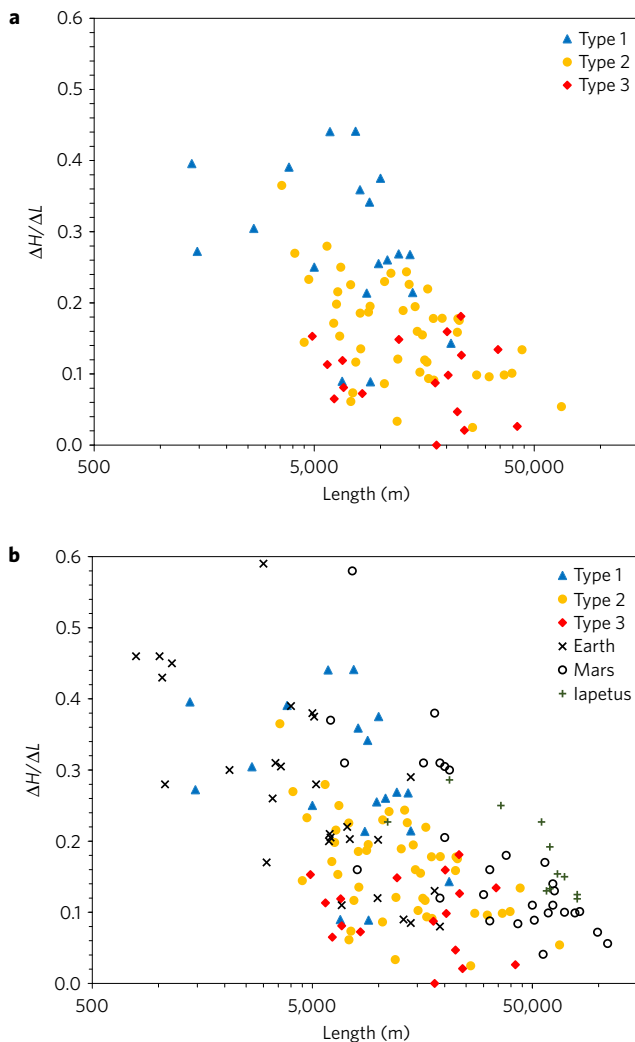


Figure 5 | $\Delta H/\Delta L$ versus length (L) of observed flows. **a**, Type 1 (blue triangles) and type 2 flows (yellow circles) have shallow $\Delta H/\Delta L$ versus L trends, whereas type 3 flows (red diamonds) show no relationship. **b**, Ceres flows are most similar to the lobate landslides on Iapetus (+ symbols; from ref. 22) and have generally lower $\Delta H/\Delta L$ values than those observed on Earth (x symbols; from ref. 23) and Mars (open circles; from ref. 23).

Ground ice also provides a context by which to understand other features on Ceres. There are many crater walls, floors and ejecta deposits that contain high-albedo features, which could be deposits left by sublimation (for example, ref. 12). Many craters have melted floors that could be produced by melting subsurface ice, and slumping or ponding of material may be another form of ice-driven mass wasting (Supplementary Information). Because Ceres is significantly warmer than icy moons, any melt reservoirs formed by impact will have a protracted lifetime, possibly promoting permafrost-style behaviour. The presence of ice in Ceres' crust suggests that water ice may indeed be common in the as-yet unexplored outer asteroid belt, and this reservoir of water represents a potential source of Earth's primordial water and a possible resource for mining of asteroids. It also blurs the compositional distinction between (rocky) asteroids and (volatile-rich) comets.

Methods

Methods, including statements of data availability and any associated accession codes and references, are available in the online version of this paper.

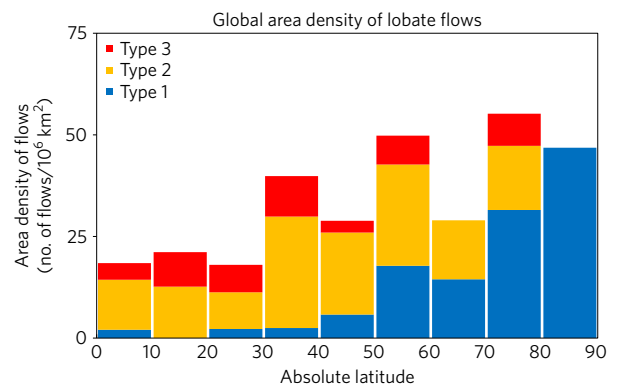


Figure 6 | Global area density of type 1 (blue bars), type 2 (yellow bars) and type 3 (red bars) flows. The areal density of surface flows on Ceres increases with increasing latitude, in particular for type 1 flows.

Received 10 June 2016; accepted 16 March 2017;
published online 17 April 2017

References

- Lebofsky, L. A., Feierberg, M. A., Tokunaga, A. T., Larson, H. P. & Johnson, J. R. The 1.7- to 4.2-micron spectrum of asteroid 1 Ceres—evidence for structural water in clay minerals. *Icarus* **48**, 453–459 (1981).
- Rivkin, A. S. *et al.* in *The Dawn Mission to Minor Planets 4 Vesta and 1 Ceres* (eds Russell, C. T. & Raymond, C. R.) 95–116 (Springer, 2012).
- De Sanctis, M. C. E. *et al.* Ammoniated phyllosilicates with a likely outer Solar System origin on (1) Ceres. *Nature* **528**, 241–244 (2015).
- Thomas, P. C. *et al.* Differentiation of the asteroid Ceres as revealed by its shape. *Nature* **437**, 224–226 (2005).
- McCord, T. B. & Sotin, C. Ceres: evolution and current state. *J. Geophys. Res.* **110**, E05009 (2005).
- Castillo-Rogez, J. C. & McCord, T. B. Ceres' evolution and present state constrained by shape data. *Icarus* **205**, 443–459 (2010).
- Zolotov, M. Y. On the composition and differentiation of Ceres. *Icarus* **204**, 183–193 (2009).
- Park, R. S. *et al.* A partially differentiated interior for (1) Ceres deduced from its gravity field and shape. *Nature* **537**, 515–517 (2016).
- Prettyman, T. *et al.* Extensive water ice within Ceres' aqueously altered regolith: evidence from nuclear spectroscopy. *Science* **15**, aah6765 (2016).
- A'Hearn, M. F. & Feldman, P. D. Water vaporization on Ceres. *Icarus* **98**, 54–60 (1992).
- Küppers, M. *et al.* Localized sources of water vapour on the dwarf planet (1) Ceres. *Nature* **505**, 525–527 (2014).
- Nathues, A. *et al.* Sublimation in bright spots on (1) Ceres. *Nature* **528**, 237–240 (2015).
- Combe, J.-P. *et al.* Detection of local H₂O exposed at the surface of Ceres. *Science* **353**, aaf3010 (2016).
- Sierks, H. *et al.* The Dawn Framing Camera. *Space Sci. Rev.* **163**, 263–327 (2011).
- Hiesinger, H. *et al.* Cratering on dwarf planet Ceres: implications for its interior and evolution. *Science* **353**, aaf4759 (2016).
- Buzckowski, D. *et al.* The geomorphology of Ceres. *Science* **353**, aaf4332 (2016).
- Bland, M. T. *et al.* Composition and structure of the shallow subsurface of Ceres as revealed by crater morphology. *Nat. Geosci.* **9**, 538–542 (2016).
- Fanaleand, F. P. & Salvail, J. R. The water regime of Asteroid (1) Ceres. *Icarus* **82**, 97–110 (1989).
- Schorghofer, N. The lifetime of ice on Main Belt Asteroids. *Astrophys. J.* **682**, 697–705 (2008).
- Hayne, P. O. & Aharonson, O. Thermal stability of ice on Ceres with rough topography. *J. Geophys. Res.* **120**, 1567–1584 (2015).
- Krohn, K. *et al.* Mass movement on Vesta at steep scarps and crater rims. *Icarus* **244**, 120–132 (2014).
- Singer, K. N., McKinnon, W. B., Schenk, P. M. & Moore, J. M. Massive ice avalanches on Iapetus mobilized by friction reduction during flash heating. *Nat. Geosci.* **5**, 574–578 (2012).
- Malin, M. C. Mass movements on Venus: preliminary results from Magellan cycle 1 observations. *J. Geophys. Res.* **97**, 16337–16352 (1992).
- Holt, J. *et al.* Radar sounding evidence for buried glaciers in the southern mid-latitudes of Mars. *Science* **322**, 1235–1238 (2008).
- Lucchitta, B. K. Valles Marineris, Mars, wet debris flows and ground ice. *Icarus* **72**, 411–429 (1987).

26. DeBlasio, F. V. Landslides in Valles Marineris (Mars): a possible role of basal lubrication by sub-surface ice. *Planet. Space Sci.* **59**, 1384–1392 (2011).
27. Haerberli, W. *et al.* Permafrost creep and rock glacier dynamics. *Perm. Periglac. Process.* **17**, 189–214 (2006).
28. White, S. E. Rock glaciers and block fields, review and new data. *Quart. Res.* **6**, 77–97 (1976).
29. Humlum, O. The geomorphic significance of rock glaciers: estimates of rock glacier debris volumes and headwall recession rates in West Greenland. *Geomorphology* **35**, 41–67 (2000).
30. Mouginiis-Mark, P. Ejecta emplacement and modes of formation of martian fluidized ejecta craters. *Icarus* **45**, 60–76 (1981).
31. Senft, L. E. & Stewart, S. T. Impact crater formation in icy layered terrains on Mars. *Met. Planet. Sci.* **43**, 1993–2013 (2008).
32. Boyce, J., Barlow, N., Mouginiis-Mark, P. & Stewart, S. Rampart craters on Ganymede: their implications for fluidized ejecta emplacement. *Met. Planet. Sci.* **45**, 638–661 (2010).
33. Legros, F. The mobility of long-runout landslides. *Eng. Geol.* **63**, 301–331 (2002).
34. Ancey, C. Plasticity and geophysical flows: a review. *J. Non-Newton. Fluid Mech.* **142**, 4–35 (2007).
35. Weertman, J. Creep deformation of ice. *Annu. Rev. Earth Planet. Sci.* **11**, 215–240 (1983).
36. Durham, W. B., Kirby, S. H. & Stern, L. A. Creep of water ices at planetary conditions: a compilation. *J. Geophys. Res.* **102**, 16293–16302 (1997).
37. Watkins, J. A., Ehlmann, B. L. & Yin, A. Long-runout landslides and the long-lasting effects of early water activity on Mars. *Geology* **43**, 107–110 (2015).
38. Marchi, S. *et al.* High-velocity collisions from the lunar cataclysm recorded in asteroidal meteorites. *Nat. Geosci.* **6**, 307 (2013).

Acknowledgements

The authors recognize the incredible efforts of the full Dawn science and operations teams. Dawn's mission is managed by JPL for NASA's Science Mission Directorate in Washington. Dawn is a project of the directorate's Discovery Program, managed by NASA's Marshall Space Flight Center in Huntsville, Alabama. UCLA is responsible for overall Dawn mission science. Orbital ATK Inc., in Dulles, Virginia, designed and built the spacecraft. The German Aerospace Center, Max Planck Institute for Solar System Research, Italian Space Agency and Italian National Astrophysical Institute are international partners on the mission team.

Author contributions

B.E.S. conceived of the paper, organized the Dawn Ground Ice working group, wrote the paper, and is an associate of the Dawn Framing Camera Team. K.H.G.H., H.T.C., J.E.C.S., T.P. and J.D.L. analysed images and provided figures. A.N. leads the Dawn Framing Camera team. The remaining authors planned observations, provided discussion and/or analysis, and helped revise the paper.

Additional information

Supplementary information is available in the [online version of the paper](#). Reprints and permissions information is available online at www.nature.com/reprints. Publisher's note: Springer Nature remains neutral with regard to jurisdictional claims in published maps and institutional affiliations. Correspondence and requests for materials should be addressed to B.E.S.

Competing financial interests

The authors declare no competing financial interests.

Methods

Data availability. The authors declare that all data supporting the findings of this study are available within the NASA Planetary Data System Small Bodies Node: http://sbn.pds.nasa.gov/data_sb/missions/dawn/index.shtml. Any additional information needed may be requested from the corresponding author.